

Effects of Fibroblast Growth Factor 2 on Burn Injury and Repair Process: Analysis Using a Refined Mouse Model

Kensaku Hishida MD*
 Sonoko Hatano, PhD†
 Hiroshi Furukawa, MD, PhD*
 Kazuhisa Yokoo, MD, PhD*
 Hideto Watanabe, MD, PhD†

Background: Burn injury is one of the most debilitating traumas, which induces multiple organ dysfunctions, resulting in high levels of morbidity and mortality. Fibroblast growth factor 2 (FGF2) has been applied to burn injury, whose precise mechanisms underlying facilitating the healing have not been fully understood. Although various animal models have been developed in pigs, rabbits, rats, and mice, no mouse model that creates burns consistent in their extent and depth have not been developed. Here, we developed a mouse burn model, and investigated details of the burn process, and elucidated the mechanisms of FGF2 effects.

Methods: A device with an 8-mm metal probe and a temperature controller was developed, which controls the temperature of the probe. Using the device, 1 or 2 of full-thickness burn injuries were generated on the back under catagen/telogen of 6-month-old C57BL/6 male mice. After 24 hours, FGF2 or phosphate-buffered saline was injected into the injured region, and at days 3, 5, and 7, histological and immunohistochemical analysis was performed to observe the injury and repair process.

Results: The device constantly generated a mouse full-thickness burn injury. The repair was initiated on the bottom of the burn as well as the margin. Local treatment with FGF2 displayed higher levels of immunostaining for both CD31+ and alpha-smooth muscle actin.

Conclusions: The device we developed is useful to generate a mouse burn injury model. FGF2 facilitates tissue repair with an increased number of both CD31+ and α SMA+ cells. (*Plast Reconstr Surg Glob Open* 2020;8:e2757; doi: 10.1097/GOX.0000000000002757; Published online 10 April 2020.)

INTRODUCTION

Burn injury is one of the most debilitating traumas, which induces multiple organ dysfunctions, resulting in high levels of morbidity and mortality. The World Health Organization has reported that 180,000 deaths every year are caused by burns. Especially, burns of large surface areas cause systemic inflammatory responses and impairment of immune systems.¹⁻³ Prolonged inflammatory responses

with high levels of cytokines and inflammatory mediators lead to a serious condition termed systemic inflammatory response syndrome, and eventually to multiple organ dysfunction syndrome.

Current treatments for burn injury include split-thickness skin graft, full-thickness skin graft, and applying artificially cultured epithelial sheets.⁴⁻⁸ For stage II burns, fibroblast growth factor 2 (FGF2) is applied to burns as well as skin ulcers.⁹⁻¹⁵

As the injury and repair process of burns involves various cell types and the extracellular matrix molecules, in vitro models are limited to capture all the aspects of burn pathophysiology, and therefore in vivo models are desirable. To date, several animal models for thermal injury have been developed,¹⁶ using pigs,^{17,18} rabbits,¹⁹ rats,²⁰⁻²² and mice.²³⁻²⁵ Out of these animals, the mouse has several advantages for the burn injury model. First, mice are less expensive and easy to prepare an adequate number for the experiments. Second, their healing occurs more rapidly than other animals. Third, an increasing number of genetically engineered mice are available, which leads to

From the *Department of Plastic and Reconstructive Surgery, Aichi Medical University, Aichi, Japan; and †Institute for Molecular Science of Medicine, Aichi Medical University, Aichi, Japan.

Supported by JSPS KAKENHI grant numbers 25293096 and 18H02646.

Received for publication August 8, 2019; accepted February 11, 2020.

Copyright © 2020 The Authors. Published by Wolters Kluwer Health, Inc. on behalf of The American Society of Plastic Surgeons. This is an open-access article distributed under the terms of the [Creative Commons Attribution-Non Commercial-No Derivatives License 4.0 \(CCBY-NC-ND\)](https://creativecommons.org/licenses/by-nc-nd/4.0/), where it is permissible to download and share the work provided it is properly cited. The work cannot be changed in any way or used commercially without permission from the journal.

DOI: 10.1097/GOX.0000000000002757

Disclosure: The authors have no financial interest to declare in relation to the content of this article.

understanding the detailed process of tissue damage and repair. Fourth, the mouse immune system is well characterized, and various assay systems and antibodies are available.¹⁶ In contrast, the major drawback is the differences in healing process in mice from humans. In mice, healing occurs primarily through wound contraction. In addition, mouse fibroblasts may have different characteristics since mice do not form keloid or hypertrophic scars. Furthermore, recent studies have revealed differences in transcriptional landscapes²⁶ and types of senescence between human and mouse.²⁷ With adequate understanding of these differences, mouse burn models are useful for elucidating the mechanisms of burn injury and repair. However, no mouse model that creates burns consistent in their extent and depth has not been developed.

Here, we developed a mouse burn model and investigated details of the burn process. Furthermore, we examined the effects of FGF2 clinically applied to burn injury and found that FGF2 substantially facilitates the repair of burns, as observed in humans.

MATERIALS AND METHODS

Generation of Burns

This study was approved by the Animal Ethics Committee of Aichi Medical University. Previously, several mouse burn models were developed and applied, including ethanol flame burn,²⁸ exposing 90°C hot water using a template with a 1 × 2 cm opening²⁵ or one with 4.5 × 1.8 cm,²⁹ exposing the skin to 60°C hot water for 18 seconds generating a wound of 10 cm².²⁹ A device was developed that controls temperature, time and pressure of contact and applied to rats.²² To constantly generate burns with the same extent of injury, a device was developed as follows. A temperature controller (TS-K; AS ONE, Osaka, Japan) and an electric branding iron (200 W; Yazawa Science, Aichi, Japan) were purchased. A flat 8-mm diameter metal was installed to the tip of the iron. A lead of the thermostat was fixed at a 5-mm distance from the tip of the metal (Fig. 1). The temperature became stable about 10 minutes after turning on the machine. When applied to male C57BL/6 mice at the age of 6 months, placing the probe at 90°C for 9 seconds gave the most appropriate level of burn. Interestingly the probe at lower or higher temperatures did not provide constant degree of burns. Then, we generated burns with the condition as above. After a series of experiments, we confirmed generation of 2 burns in a mouse shows similar levels of burns to that of 1 in a mouse. After that, we generated 2 burns in a mouse.

Gross Appearances

Burns were observed every day up to day 14, and at days 3, 5, 7, 10, and 14, mice were anesthetized or euthanized, and photos were taken using a camera (Nikon D3300, Nikon, Tokyo, Japan).

Histology and Immunohistochemistry

At days 2, 5, and 7 after generation of burns, skin fragment of 35 × 25 mm containing the burn in the center

was excised with whole thickness. When the bottom of the burn adhered to the subcutaneous muscle, the muscle was included. Then the excised skin was placed onto a nitrocellulose membrane (BioRad, Tokyo, Japan) to avoid shrinkage and distortion, fixed in 4% paraformaldehyde/phosphate-buffered saline (PBS) for 24 hours, and embedded in paraffin. Then, section slides of 4 μm thickness were prepared, deparaffinized in xylene, rehydrated in an ethanol gradient, and briefly washed with dH₂O, and stained for hematoxylin and eosin. For immunostaining, antigen retrieval by autoclaving for 20 minutes with 0.5 M Tris-HCl buffer, pH 8.8, 1 mM EDTA was performed for CD31. Section slides were treated with 0.2% Triton X-100 for 15 minutes for alpha-smooth muscle actin (αSMA). Then, slides were treated with blocking solution (Dako, Japan, Tokyo) at room temperature for 1 hour, and incubated with the following primary antibodies at 4°C overnight: anti-CD31 (1:50; Abcam, Tokyo, Japan), anti-αSMA (1:250; Sigma-Aldrich, Tokyo, Japan). After washing, slides were incubated with goat anti-mouse AlexaFluor594 (1:1000; Invitrogen, Tokyo, Japan) or goat anti-rabbit AlexaFluor594 (1:1000; Invitrogen) for fluorescent detection. After staining with 1 μg/mL 4',6-diamidino-2-phenylindole (DAPI; Wako, Osaka, Japan) for 10 minutes, followed by 3 washes with PBS, samples were mounted with aqueous mounting medium and observed under a fluorescence microscope (BZ-9000; Keyence).

Fibroblast Growth Factor 2 Treatment

Twenty-four hours after generation of the burn, 100 μL of Trafermin (Kaken Pharmaceuticals, Tokyo, Japan) at a concentration of 100 μg/mL or PBS as control was injected into marginal areas of the burn (n = 15 and 16 each for day 3 and n = 8 and 9 each for day 5, respectively). To quantify the levels of immunostaining, photos of four areas were taken, and the pixels were measured using a histogram of Photoshop application. Relative areas of each staining were calculated by positive pixels/total pixels (positive pixels + negative) pixels. Quantification was performed on images taken with same exposure setting and without post-image processing.

Statistical Analysis

Data are presented as mean ± SD. Statistical analyses were performed with post hoc tests (Bonferroni) using analysis of variance. Probability values of 0.05 were considered statistically significant.

RESULTS

We developed a device, which maintains the temperature of the probe (Fig. 1A). After a series of experiments, the condition was optimized to be 90°C for 9 seconds. Under this condition, mice developed a certain level of burns in their back constantly. Treatment for longer than 9 seconds often led to death (3 deaths out of 5), whereas less than 8 seconds generated a reduced level of burns, which was cured within a few days. Application for mice with different ages revealed that mice of 6 months of age are appropriate. Younger mice at 12 weeks provided

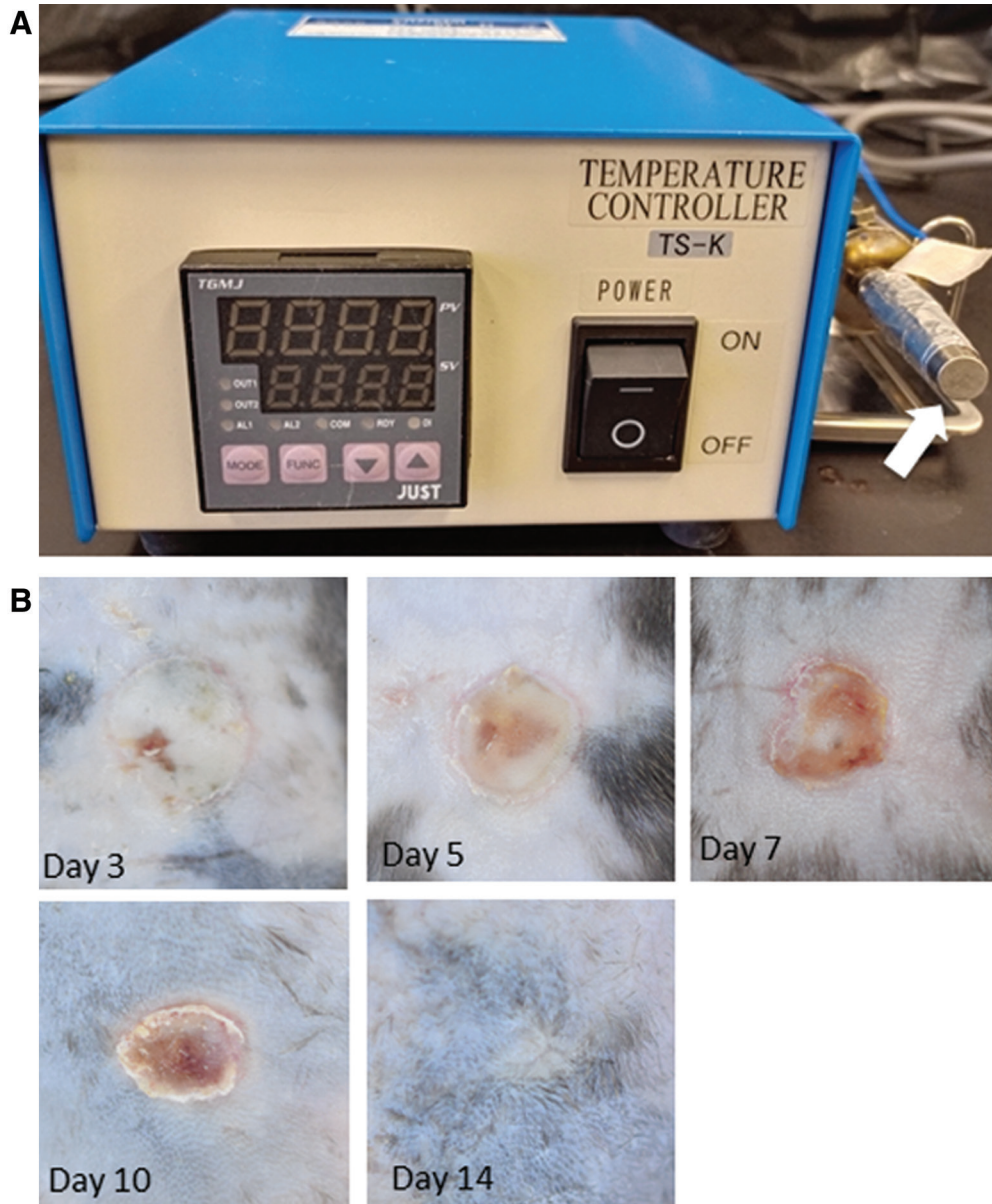


Fig. 1. Device and gross appearances of burns. The device with a probe (white arrow) of 8 mm in diameter attached with a thermometer is shown (A). Burn injury was grossly observed, and photographs were taken at days indicated. Representative photograph panels of burns (out of 5, each) at days indicated after burn are shown (B).

smaller areas for the generation of burns and increased the death rate (2 deaths out of 4). Older mice disturbed generation of constant levels of burns, as tested for up to 12 mice, presumably due to variable volumes of subcutaneous fat.

In mice, the structure of the dermis and the width of the subcutaneous space change, depending on the hair cycle.³⁰ Under the anagen phase, while hairs develop, hair follicles extend deeply into subcutaneous region, generating a wide space between dermis and muscular layer. In contrast, under the telogen phase, when hair follicles wither, the space decreases, and dermis becomes thinner. In C57BL/6, the skin under anagen is gray and is easily

recognized by gross appearances. As the hair cycle is not synchronized, gray patches are often observed on the back of mice after shaving hairs. We found that burn injury generated on anagen is milder in general than that on catagen and telogen, and more importantly, that it exhibits broader variations of burn levels. Based on the results obtained by our preliminary experiments, we concluded that application to catagen/telogen phase on the back after shaving constantly generates a certain level of burns.

By gross appearances, the region immediately after the burn was hardly appreciable. At day 3, the lesion was smooth with a clear margin. At day 5, it was partially reddish, which became broader at day 7. At day 10, the lesion

was shrunk and the surface appeared dry with hard crust. At day 14, the lesion was almost cured (Fig. 1B).

Histologically, dermis under the burn region exhibited swelling and blurring of collagen fibers and massive necrosis of fibroblasts at day 1 (Fig. 2A), demonstrating full-thickness burn damage. At day 2, granulation appeared on both the bottom and the margin of the burned area, which became remarkable at day 3 (Fig. 2B). At day 7, granulation developed especially at the bottom (Fig. 2C) and the margin of the burn region (Fig. 2D), which was confirmed by immunostaining for α SMA (Fig. 2E, F).

Clinically, FGF2 is commonly applied to the treatment of skin ulcer and burn injury.⁹⁻¹⁵ We examined the effects of FGF2 on healing of burn injury. At day 3 after burn, histological analysis demonstrated increased thickness of overall skin and an increased number of cells, especially on the bottom region in FGF2-treated samples. By immunostaining, whereas FGF2 treated samples did not reveal

increased CD31+ levels with a statistical significance at day 3 (mean \pm SD, a.u., 1.00 ± 0.59 and 1.02 ± 0.64 , for PBS and FGF2-treated samples, respectively, $P = 0.63$), they did at day 5 (mean \pm SD, a.u., 1.00 ± 1.25 and 1.48 ± 1.48 , for PBS and FGF2-treated samples, respectively, $P = 0.018$). Similarly, FGF2-treated samples did not show increased levels of α SMA at day 3 (mean \pm SD, a.u., 1.00 ± 0.4 and 1.04 ± 0.39 , for PBS and FGF2-treated samples, respectively, $P = 0.38$), they did at day 5 (mean \pm SD, a.u., 1.00 ± 1.25 and 1.32 ± 1.84 , for PBS and FGF2-treated samples, respectively, $P = 0.022$) (Fig. 3). These results suggest that FGF2 facilitates granulation by up-regulating the proliferation of endothelial cells and fibroblasts.

DISCUSSION

In this study, we established a repeatable and reliable burn injury model in mice for the first time. This model is a powerful tool, as it can be applied to genetically modified

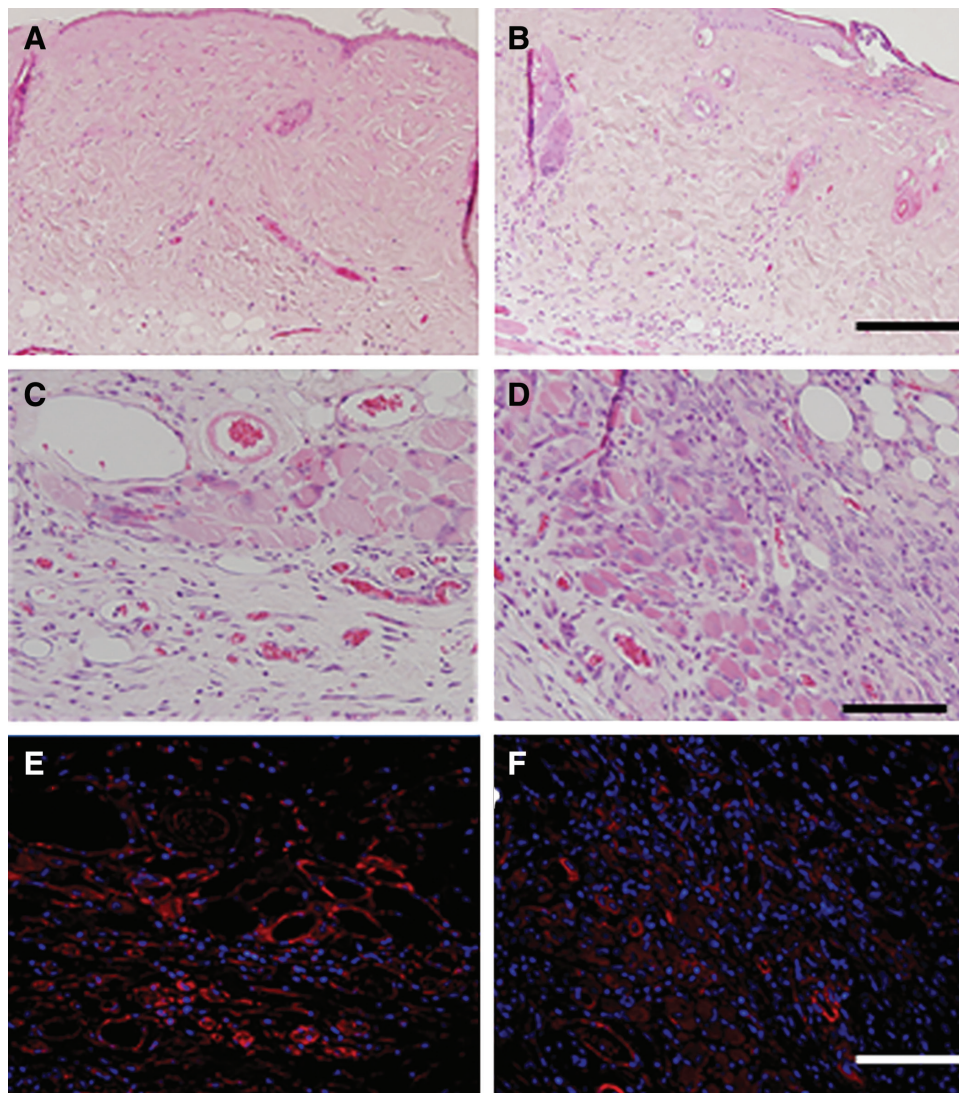


Fig. 2. Histology and immunohistochemistry. H&E staining patterns of day 1 (A), day 3 (B) and day 7 (C, bottom region; D, margin) are shown. Immunostaining patterns for α SMA, corresponding to panels C and D, are shown in E and F (A, B, bar = 200 μ m; C, D, bar = 40 μ m). H&E, hematoxylin and eosin.

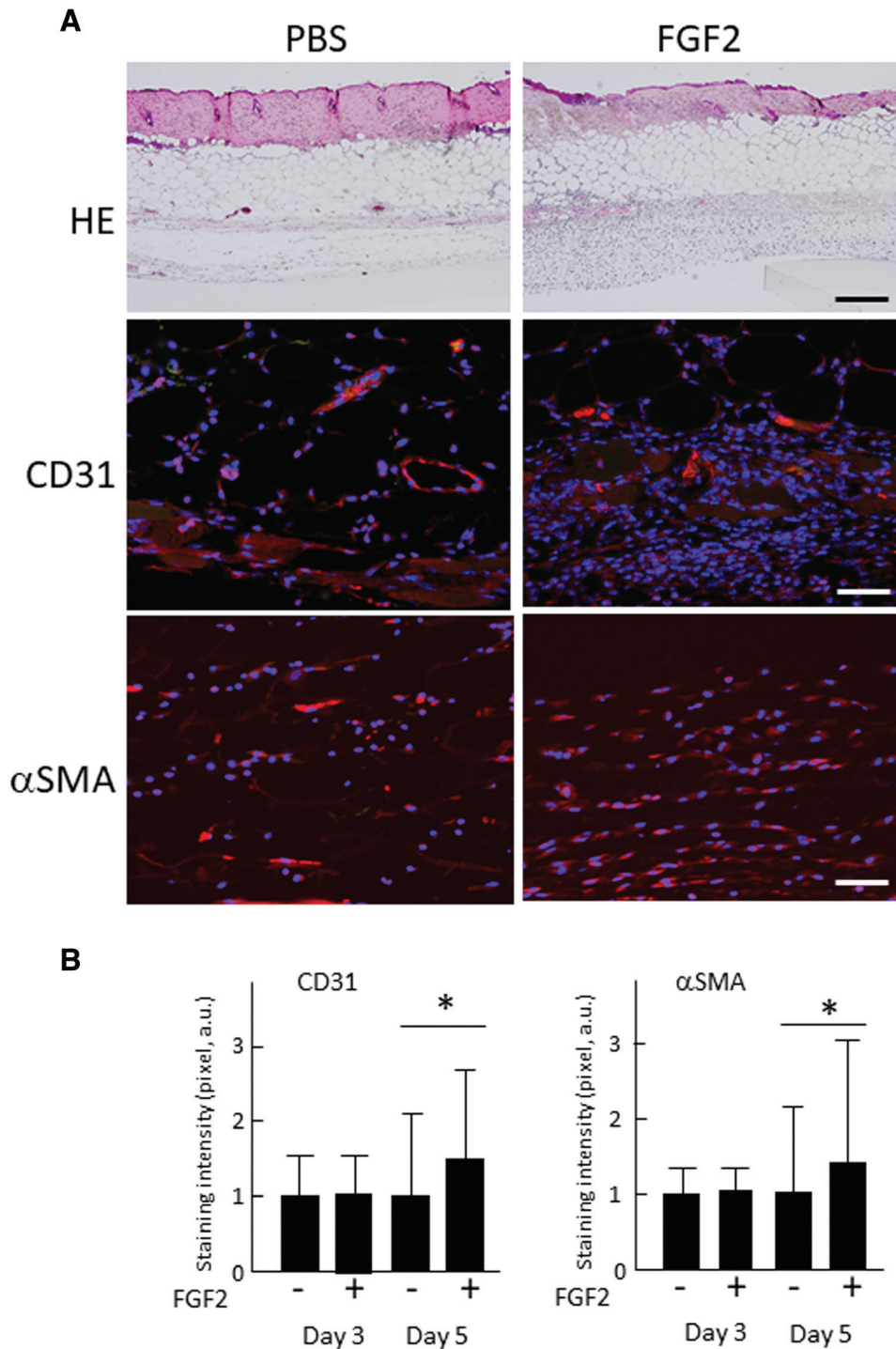


Fig. 3. Effects of FGF2 on the healing of burns. H&E staining patterns at day 3 are shown (A, upper panels). Note that FGF2-treated skin is thickened with edema and an increased number of cells. Immunostaining patterns for CD31 (A, second panels), αSMA (A, third panels) are shown. Note that an increase in CD31- and αSMA-positive cells in FGF2-treated skin. The quantification data of CD31 and αSMA are presented as graphs (B). Asterisk represents $P < 0.05$. H&E, hematoxylin and eosin.

mice. Several therapeutic approaches can be evaluated on each repair process, as we demonstrated for FGF2.

Whereas our mouse burn model is applicable to various types of genetically engineered mice, we found some

limitations in this model, when compared with human burns. In humans, burns exhibit zones of coagulation, stasis, and hyperemia. There, re-perfusion in the zone of stasis is critical for better healing.³¹ In mice, burn regions

do not exhibit clear zones like humans. This could be simply due to small volumes of the defects. Also, strong contractile forces shrink the defects during the repair process. Whereas the severity of burns is evaluated by gross appearances in humans, gross appearances of mouse burns do not always co-relate with histopathological observations. Whereas the same histological patterns were obtained, parameters such as redness, ulcer, and crust varied among individuals. Interestingly, regeneration of mouse burns occurs in both the marginal and bottom regions, whereas burn regeneration from the bottom region does not occur in a full-thickness burn of humans.

In mice, a wound with a full-thickness skin defect by 8-mm punch biopsy heals within a week. Compared with wound healing, that from burns takes longer, probably due to the presence of crust and regions of coagulation necrosis. The presence of crust appears to disturb contraction of wound and delays re-epithelization. We noticed that tissue repair was more active on the bottom of the lesion rather than the marginal areas, which is distinct from wound healing. The necrotic tissue remaining on the margin may disturb granulation in the burn wound.

We confirmed the effects of FGF2 on the healing of burns in mice. In a wound-healing model, FGF2 increases collagen biosynthesis, cell proliferation and angiogenesis, promoting granulation.³² In the same model using diabetic mice, FGF2 induces the infiltration of a large number of macrophages, monocytes and fibroblasts, and restores the inflammatory response in diabetic conditions.³³ However, in the healing process, the target cells and the mechanism by which FGF2 exert function were not clearly understood. Our immunostaining results show an increased number of α SMA+ and CD31 cells especially on the bottom of the full-thickness defects of FGF2-treated samples, demonstrating that FGF2 upregulates proliferation of fibroblasts/myofibroblasts and endothelial cells facilitating granulation. The wound healing process involves several growth factors with different functions, including platelet-derived growth factors, transforming growth factor β , epidermal growth factor and vascular endothelial growth factor.³⁴ Our burn injury model is useful for evaluation of treatment of burn injury with these growth factors, as well as new therapeutic substances.

Hideto Watanabe, MD, PhD

Institute for Molecular Science of Medicine

Aichi Medical University

1-1 Yazakokarimata, Nagakute

Aichi 480-1195, Japan

E-mail: wannabee@aichi-med-u.ac.jp

References

- Ogura H, Hashiguchi N, Tanaka H, et al. Long-term enhanced expression of heat shock proteins and decelerated apoptosis in polymorphonuclear leukocytes from major burn patients. *J Burn Care Rehabil.* 2002;23:103–109.
- Hoover L, Bochicchio GV, Napolitano LM, et al. Systemic inflammatory response syndrome and nosocomial infection in trauma. *J Trauma.* 2006;61:310–316; discussion 316.
- Sauaia A, Moore FA, Moore EE, et al. Early risk factors for postinjury multiple organ failure. *World J Surg.* 1996;20:392–400.
- Hermans MHE. An introduction to burn care. *Adv Skin Wound Care.* 2019;32:9–18.
- Chua AWC, Khoo YC, Truong TTH, et al. From skin allograft coverage to allograft-micrograft sandwich method: a retrospective review of severe burn patients who received conjunctive application of cultured epithelial autografts. *Burns.* 2018;44:1302–1307.
- Liu HF, Zhang F, Lineaweaver WC. History and advancement of burn treatments. *Ann Plast Surg.* 2017;78(2 suppl 1):S2–S8.
- Singh M, Nuutila K, Collins KC, et al. Evolution of skin grafting for treatment of burns: reverdin pinch grafting to tanner mesh grafting and beyond. *Burns.* 2017;43:1149–1154.
- Orgill DP, Ogawa R. Current methods of burn reconstruction. *Plast Reconstr Surg.* 2013;131:827e–836e.
- Mitsukawa N, Higaki K, Ito N, et al. Combination treatment of artificial dermis and basic fibroblast growth factor for skin defects: a histopathological examination. *Wounds.* 2016;28:158–166.
- Hayashida K, Akita S. Quality of pediatric second-degree burn wound scars following the application of basic fibroblast growth factor: results of a randomized, controlled pilot study. *Ostomy Wound Manage.* 2012;58:32–36.
- Akita S, Akino K, Imaizumi T, et al. Basic fibroblast growth factor accelerates and improves second-degree burn wound healing. *Wound Repair Regen.* 2008;16:635–641.
- O’Goshi K, Tagami H. Basic fibroblast growth factor treatment for various types of recalcitrant skin ulcers: reports of nine cases. *J Dermatolog Treat.* 2007;18:375–381.
- Muneuchi G, Suzuki S, Moriue T, et al. Combined treatment using artificial dermis and basic fibroblast growth factor (bfgf) for intractable fingertip ulcers caused by atypical burn injuries. *Burns.* 2005;31:514–517.
- Gibran NS, Isik FF, Heimbach DM, et al. Basic fibroblast growth factor in the early human burn wound. *J Surg Res.* 1994;56:226–234.
- Nunes QM, Li Y, Sun C, et al. Fibroblast growth factors as tissue repair and regeneration therapeutics. *PeerJ.* 2016;4:e1535.
- Abdullahi A, Amini-Nik S, Jeschke MG. Animal models in burn research. *Cell Mol Life Sci.* 2014;71:3241–3255.
- Petersen W, Rahmanian-Schwarz A, Werner JO, et al. The use of collagen-based matrices in the treatment of full-thickness wounds. *Burns.* 2016;42:1257–1264.
- Theunissen D, Seymour B, Forder M, et al. Measurements in wound healing with observations on the effects of topical agents on full thickness dermal incised wounds. *Burns.* 2016;42:556–563.
- Friedrich EE, Niknam-Bienia S, Xie P, et al. Thermal injury model in the rabbit ear with quantifiable burn progression and hypertrophic scar. *Wound Repair Regen.* 2017;25:327–337.
- Wiggins-Dohlvik K, Tharakan B. A rat burn injury model for studying changes in microvascular permeability. *Methods Mol Biol.* 2018;1717:93–100.
- Porumb V, Trandabăţ AF, Terinte C, et al. Design and testing of an experimental steam-induced burn model in rats. *Biomed Res Int.* 2017;2017:9878109.
- Sakamoto M, Morimoto N, Ogino S, et al. Preparation of partial-thickness burn wounds in rodents using a new experimental burning device. *Ann Plast Surg.* 2016;76:652–658.
- Maden M. Optimal skin regeneration after full thickness thermal burn injury in the spiny mouse, *Acomys cahirinus*. *Burns.* 2018;44:1509–1520.
- Brisbois EJ, Bayliss J, Wu J, et al. Optimized polymeric film-based nitric oxide delivery inhibits bacterial growth in a mouse burn wound model. *Acta Biomater.* 2014;10:4136–4142.
- Barnea Y, Carmeli Y, Kuzmenko B, et al. The establishment of a pseudomonas aeruginosa-infected burn-wound sepsis model and the effect of imipenem treatment. *Ann Plast Surg.* 2006;56:674–679.
- Lin S, Lin Y, Nery JR, et al. Comparison of the transcriptional landscapes between human and mouse tissues. *Proc Natl Acad Sci USA.* 2014;111:17224–17229.

27. Itahana K, Campisi J, Dimri GP. Mechanisms of cellular senescence in human and mouse cells. *Biogerontology*. 2004;5:1–10.
28. Stieritz DD, Holder IA. Experimental studies of the pathogenesis of infections due to *Pseudomonas aeruginosa*: description of a burned mouse model. *J Infect Dis*. 1975;131:688–691.
29. McVay CS, Velásquez M, Fralick JA. Phage therapy of *Pseudomonas aeruginosa* infection in a mouse burn wound model. *Antimicrob Agents Chemother*. 2007;51:1934–1938.
30. Alonso L, Fuchs E. The hair cycle. *J Cell Sci*. 2006;119(pt 3):391–393.
31. Rose LF, Chan RK. The burn wound microenvironment. *Adv Wound Care (New Rochelle)*. 2016;5:106–118.
32. Okumura M, Okuda T, Nakamura T, et al. Effect of basic fibroblast growth factor on wound healing in healing-impaired animal models. *Arzneimittelforschung*. 1996;46:547–551.
33. Tanaka E, Ase K, Okuda T, et al. Mechanism of acceleration of wound healing by basic fibroblast growth factor in genetically diabetic mice. *Biol Pharm Bull*. 1996;19:1141–1148.
34. Barrientos S, Stojadinovic O, Golinko MS, et al. Growth factors and cytokines in wound healing. *Wound Repair Regen*. 2008;16:585–601.